

HE-LHC vs. HL-LHC Potential for Supersymmetry Discovery

Amin Aboubrahim

Northeastern University
Boston, MA, USA

Workshop on the physics of HL-LHC, and
perspectives at HE-LHC

CERN, Switzerland
June 18-20, 2018

Table of Contents

- 1 Introduction
- 2 Chargino Coannihilation in SUGRA Models
- 3 SUGRA benchmarks and sparticle spectrum
- 4 Gluginos and Electroweakinos at the HL-LHC vs. HE-LHC
- 5 Conclusion

Introduction

- In models where the LSP is bino-like, coannihilation is needed to deplete the relic density to $\Omega h^2 = 0.1197 \pm 0.0022$ [Planck Collaboration, arXiv:1502.01589 [astro-ph.CO]]
- Coannihilation requires the mass gap between the LSP and the NLSP be small (typically $\lesssim 20$ GeV)
- For $\tilde{\chi}_i \tilde{\chi}_j \rightarrow SM$, the relic density is controlled by the ratio

$$\delta_i = \frac{n_i^{eq}}{n^{eq}} = \frac{g_i (1 + \Delta_i)^{3/2} e^{-\Delta_i x}}{\sum_j g_j (1 + \Delta_j)^{3/2} e^{-\Delta_j x}},$$

where $\Delta_i = (m_i - m_1)/m_1$, g_i are the degrees of freedom of χ_i and $x = m_1/T$. The relic density involved in the integral

$$J_{x_f} = \int_{x_f}^{\infty} x^{-2} \langle \sigma_{eff} v \rangle dx$$

SUGRA models

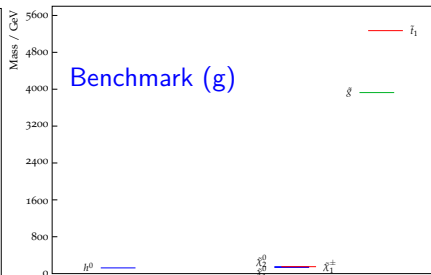
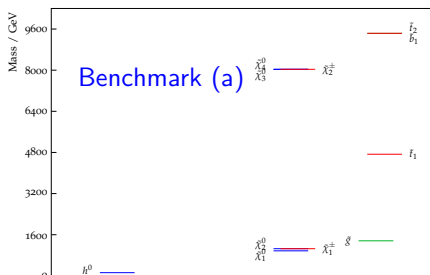
- In previous works, stop^1 , gluino^2 and stau^3 coannihilation have been discussed
 - ¹[B. Kaufman, P. Nath, B. Nelson, A. Spisak, arXiv:1509.02530v2 [hep-ph]]
 - ²[P. Nath, A. Spisak, arXiv:1603.04854v2 [hep-ph]]
 - ³[A. Aboubrahim, P. Nath, and A. Spisak, arXiv:1704.04669 [hep-ph]]
- Here we extend the study to chargino coannihilation models. To achieve chargino coannihilation we need non-universal SUGRA:
 $m_0, A_0, m_1, m_2, m_3, \tan \beta, \text{sign}(\mu)$
- For the case of heavy gluinos and lighter electroweakinos one has $m_3 \gg m_1 > m_2$ while for electroweakinos and gluinos with masses $\mathcal{O}(1)$ TeV one has $m_1 > m_2 \gg m_3$

- The ten benchmark points satisfying the Higgs boson mass and relic density constraints

Model	m_0	A_0	m_1	m_2	m_3	$\tan \beta$
(a)	13998	30376	2155	1249	556	28
(b)	9528	22200	2281	1231	573	34
(c)	9288	20898	2471	1411	620	40
(d)	28175	62830	2634	1541	751	41
(e)	20335	44737	2459	1133	550	24
(f)	22648	50505	2700	1585	675	15
(g)	16520	37224	385	274	1685	16
(h)	48647	106537	537	432	2583	26
(i)	14266	-28965	371	224	2984	20
(j)	41106	108520	687	599	7454	42

Sparticle mass hierarchies

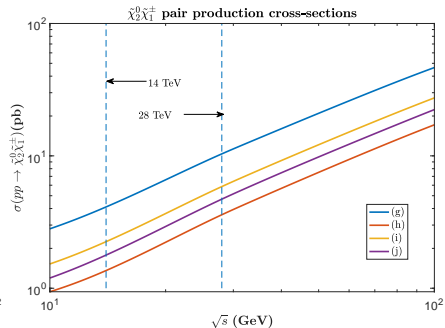
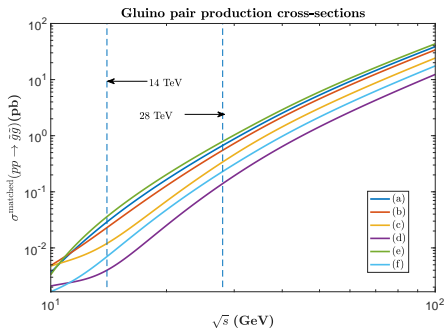
- With a small available mass gap between the LSP and the NLSP, decay products are soft. Switch on ISR and FSR
- SUGRA benchmarks (a)-(f) chosen with gluino and electroweakino masses $\mathcal{O}(1)$ TeV while points (g)-(j) have heavier gluinos and lighter electroweakinos [A. Aboubrahim, P. Nath, arXiv:1804.08642 [hep-ph]]



The 28 TeV collider: HE-LHC

- The High Energy LHC (HE-LHC) is a possible candidate as the next generation pp collider at CERN
- Uses the existing LHC ring with 16 T FCC magnets replacing the current 8.3 T ones
- Center-of-mass energy boosted to 28 TeV with a design luminosity ~ 4 times that of the HL-LHC
- This set up necessarily means that a larger part of the parameter space of supersymmetric models beyond the reach of the 14 TeV collider will be probed

- Production cross-section of $\tilde{g}\tilde{g}$ at 28 TeV is $\sim 20 - 30$ times that at 14 TeV
- An increase by ~ 2.5 folds is seen for the case of electroweakino production



• Decay BRs of the gluino, second neutralino and chargino

Model	$\tilde{g} \rightarrow \tilde{\chi}_1^0 q \bar{q}$	$\tilde{g} \rightarrow \tilde{\chi}_1^\pm q_i \bar{q}_j$ $q \in \{u, d, c, s, t, b\}$	$\tilde{g} \rightarrow \tilde{\chi}_2^0 q \bar{q}$	$\tilde{\chi}_1^\pm \rightarrow \tilde{\chi}_1^0 W^\pm$
(a)	0.66	0.29	0.05	1.0
(b)	0.33	0.53	0.13	0.32
(c)	0.63	0.33	0.04	0.33
(d)	0.48	0.40	0.12	1.0
(e)	0.36	0.63	0.01	0.25
(f)	0.73	0.20	0.07	1.0
	$\tilde{\chi}_2^0 \rightarrow \tilde{\chi}_1^0 q \bar{q}$ $q \in \{u, d, c, s\}$	$\tilde{\chi}_2^0 \rightarrow \tilde{\chi}_1^0 \ell \bar{\ell}$ $\ell \in \{e, \mu, \tau, \nu\}$	$\tilde{\chi}_1^\pm \rightarrow \tilde{\chi}_1^0 q_i \bar{q}_j$ $q \in \{u, d, c, s, b\}$	$\tilde{\chi}_1^\pm \rightarrow \tilde{\chi}_1^0 \ell^\pm \nu_\ell$ $\ell \in \{e, \mu, \tau\}$
(g)	0.88	0.12	0.67	0.33
(h)	0.84	0.16	0.67	0.33
(i)	0.68	0.32	0.67	0.33
(j)	0.94	0.06	0.67	0.33

- Signal regions (SR) used in this analysis correspond to the single lepton, two lepton (same flavor opposite sign leptons, SFOS) and the three lepton channel

- For the one lepton channel:

$$\tilde{g}\tilde{g} \rightarrow (\tilde{\chi}_1^0 q \bar{q})(\tilde{\chi}_1^\pm q_i \bar{q}_j) \text{ and } \tilde{\chi}_2^0 \tilde{\chi}_1^\pm \rightarrow (\tilde{\chi}_1^0 q \bar{q})(\tilde{\chi}_1^0 \ell^\pm \nu_\ell)$$

- For the two lepton channel (SFOS):

$$\tilde{g}\tilde{g} \rightarrow (\tilde{\chi}_1^0 q \bar{q})(\tilde{\chi}_2^0 q \bar{q}) \text{ and } \tilde{\chi}_2^0 \tilde{\chi}_1^\pm \rightarrow (\tilde{\chi}_1^0 \ell \bar{\ell})(\tilde{\chi}_1^0 q_i \bar{q}_j)$$

- For the three lepton channel:

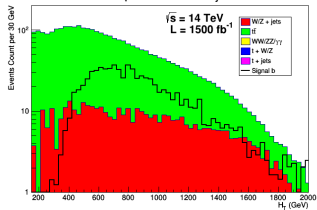
$$\tilde{g}\tilde{g} \rightarrow (\tilde{\chi}_1^\pm q_i \bar{q}_j)(\tilde{\chi}_2^0 q \bar{q}) \text{ and } \tilde{\chi}_2^0 \tilde{\chi}_1^\pm \rightarrow (\tilde{\chi}_1^0 \ell \bar{\ell})(\tilde{\chi}_1^0 \ell^\pm \nu_\ell)$$

- Each SR has two classes of selection criteria, one targeting final states from gluino decay and the other suitable for soft final states from electroweakino pair decay

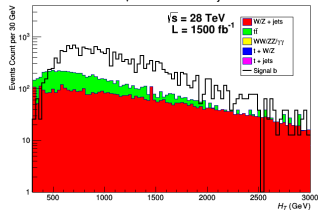
Integrated luminosities at HL-LHC vs HE-LHC

Distributions for benchmark (b)

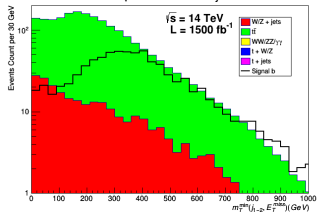
S and \sqrt{B} in the $1\ell+jets$ SR



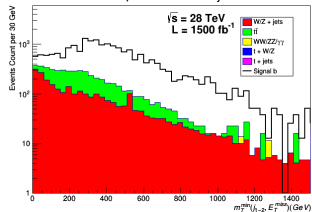
S and \sqrt{B} in the $1\ell+jets$ SR



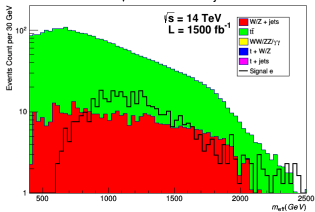
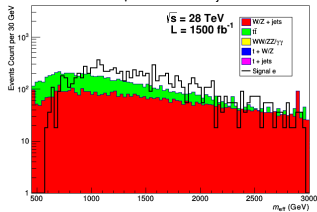
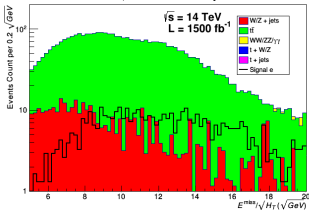
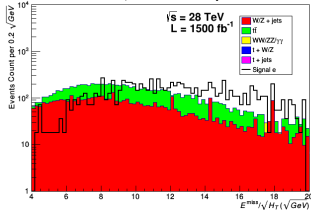
S and \sqrt{B} in the $1\ell+jets$ SR



S and \sqrt{B} in the $1\ell+jets$ SR



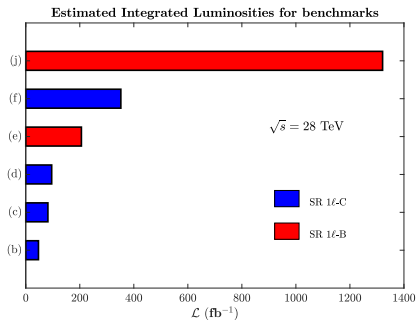
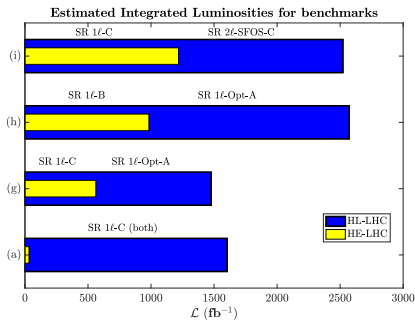
Distributions for benchmark (e)

S and \sqrt{B} in the $1\ell+jets$ SRS and \sqrt{B} in the $1\ell+jets$ SRS and \sqrt{B} in the $1\ell+jets$ SRS and \sqrt{B} in the $1\ell+jets$ SR

Estimated integrated luminosities for a 5σ discovery at HE-LHC vs HL-LHC

Model	Leading SR at 28 TeV	\mathcal{L} (fb^{-1})	Leading SR at 14 TeV	\mathcal{L} (fb^{-1})
(a)	SR-1 l -C	32	SR-1 l -C	1603
(b)	SR-1 l -C	47	SR-1 l -B	3264
(c)	SR-1 l -C	82	SR-1 l -C	7578
(d)	SR-1 l -C	96	SR-1 l -B	13035
(e)	SR-1 l -B	206	SR-1 l -A	8246
(g)	SR-2 l SFOS-A	267	SR-1 l -A	1477
(f)	SR-1 l -C	352	SR-1 l -B	38015
(h)	SR-1 l -B	983	SR-1 l -A	2572
(i)	SR-1 l -C	1218	SR-1 l -A	3131
(j)	SR-1 l -B	1321	SR-1 l -A	3484

The discovery of points (a), (g), (h) and (i) would require a run of HL-LHC for ~ 5 yr for (a) and (g), and ~ 8 yr for (h) and (i). The run period for discovery of these at HE-LHC will be ~ 2 weeks for (a), ~ 4 months for (g), ~ 1 yr for (h) and ~ 1.5 yr for (i) using the projection that HE-LHC will collect 820 fb^{-1} of data per year



Conclusion

- The parameter space satisfying the Higgs boson mass constraint mostly gives a neutralino which is bino-like. Hence coannihilation is needed to achieve the correct relic density
- Because of small mass gaps between the LSP and NLSP, supersymmetric signals arising from chargino coannihilation regions are hard to detect at colliders since the decay products are soft
- It is found that SUSY discovery at HE-LHC would take a much shorter time reducing the run period of 5-8 yr at HL-LHC to a run period of few weeks to ~ 1.5 yr at HE-LHC
- HE-LHC is a powerful tool for the discovery of supersymmetry and deserves serious consideration

BACKUP SLIDES

- The Higgs boson mass, some relevant sparticles masses and the relic density for the 10 benchmark points

Model	h^0	μ	$\tilde{\chi}_1^0$	$\tilde{\chi}_1^\pm$	\tilde{t}	\tilde{g}	$\Omega_{\tilde{\chi}_1^0}^{\text{th}} h^2$
(a)	123.7	8022	973	1056	4730	1363	0.039
(b)	125.4	6287	1023	1033	2080	1404	0.035
(c)	123.4	5588	1110	1187	2883	1510	0.048
(d)	123.5	15488	1188	1272	10032	1745	0.048
(e)	123.9	11725	948	948	6775	1329	0.020
(f)	124.4	13674	1236	1348	6976	1620	0.112
(g)	124.2	10400	134.2	150.6	5271	3927	0.121
(h)	123.7	26052	154.3	175.7	18591	5880	0.105
(i)	124.1	1146	165.2	188.9	4171	6705	0.114
(j)	125.3	29685	162.4	187.3	10405	15575	0.105

Kinematic variables

- The lepton transverse mass

$$m_T^\ell = \sqrt{2p_T^\ell E_T^{\text{miss}}(1 - \cos \Delta\phi(\ell, E_T^{\text{miss}}))}, \quad (1)$$

which is used to reduce $t\bar{t}$ and $W + \text{jets}$ backgrounds

- The ratio R defined as

$$R = \frac{E_T^{\text{miss}}}{E_T^{\text{miss}} + \sum p_T^\ell} \rightarrow 1 \quad \text{for signal due to large } E_T^{\text{miss}}. \quad (2)$$

- The effective mass, m_{eff} , is given by

$$m_{\text{eff}} = H_T + E_T^{\text{miss}} + \sum p_T^\ell. \quad (3)$$

m_{eff} tend to have values higher than the background especially in processes involving gluino pair production

Kinematics variables (cont'd)

- H_T is the scalar sum of all the jets' transverse momenta. It is important when dealing with high jet activity
- The variable $E_T^{\text{miss}} / \sqrt{H_T}$ is effective in eliminating possible multi-jet background events
- The Fox-Wolfram moments are given by

$$H_\ell = \sum_{ij} \frac{|\vec{p}_i| |\vec{p}_j|}{E_{\text{vis}}^2} P_\ell(\cos \theta_{ij}). \quad (4)$$

This event shape observable is mostly effective for hard jets which is why it is only applied to gluino pair production

Kinematics variables (cont'd)

- The ratio \mathcal{A} describes the p_T asymmetry between the two leading jets and is given by

$$\mathcal{A} = \frac{p_T(j_1) - p_T(j_2)}{p_T(j_1) + p_T(j_2)}. \quad (5)$$

This quantity is most effective when the mass gap between the NLSP and the LSP is small

- The variable M_{T2}

$$M_{T2} = \min \left[\max \left(m_T(\mathbf{p}_{T1}, \mathbf{q}_T), m_T(\mathbf{p}_{T2}, \mathbf{p}_T^{\text{miss}} - \mathbf{q}_T) \right) \right]. \quad (6)$$

This variable defined for the dilepton case is effective in reducing SM $t\bar{t}$ and WW backgrounds

The selection criteria used for the single lepton channel

Requirement	SR 1 ℓ -comp			SR 1 ℓ - \tilde{g}		
	SR-A	SR-B	SR-C	SR-A	SR-B	SR-C
$N_{\text{jets}} \geq$	2	2	2	2	2	2
E_T^{miss} (GeV) >				150	150	150
H_T (GeV)	< 250	< 250	< 250	> 600	> 600	> 600
$E_T^{\text{miss}}/\sqrt{H_T}$ (GeV $^{1/2}$) >	7	7	7	10	10	10
m_{eff} (GeV)	< 350	< 350	< 350	> 800	> 800	> 800
R >	0.6	0.7	0.85	0.7	0.8	0.85
$H_{20} <$				0.5	0.5	0.5
$p_T(j_2)$ (GeV) >				110	110	110
$p_T(j_3)$ (GeV) >				80	80	80
$p_T(j_4)$ (GeV) >				50	50	50
m_T^ℓ (GeV) >				100	100	100
$m_T^{\text{min}}(j_{1-2}, E_T^{\text{miss}})$ (GeV) >				200	200	200

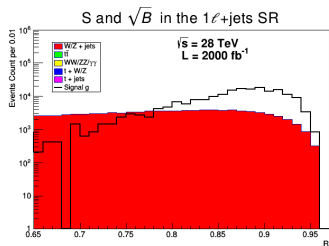
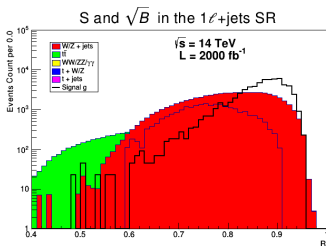
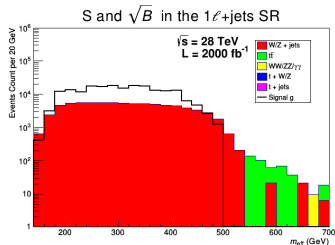
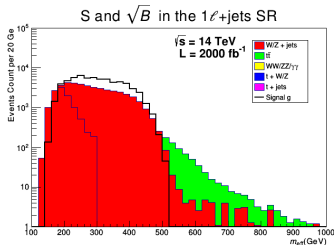
Requirement	$2l$ -SFOS-comp			$2l$ -SFOS- \tilde{g}		
	SR-A	SR-B	SR-C	SR-A	SR-B	SR-C
$N_{\text{jets}} \geq$	2	2	2	2	2	2
E_T^{miss} (GeV)	< 150	< 150	< 150	> 150	> 150	> 150
m_T^{ℓ} (GeV)	< 80	< 80	< 80	> 150	> 180	> 200
$p_T(j_1)$ (GeV)	< 90	< 90	< 90	> 120	> 120	> 120
$p_T(j_2)$ (GeV)	< 48	< 48	< 48	> 80	> 80	> 80
$R >$	0.7	0.7	0.7	0.8	0.8	0.8
$A <$	0.4	0.4	0.4			
$m_{\ell\ell}$ (GeV) <	25	25	25		Z-veto	
H_T (GeV)	< 190	< 190	< 190	> 500	> 500	> 500
m_{eff} (GeV) >	180	180	180	900	900	900
m_{eff} (GeV) <	400	400	400			
$\Delta R_{\ell\ell}$ (rad) <	0.4	1.0	2.5			
$M_{T_2}^{\text{dijet}}$ (GeV) >				700	700	700
$M_{T_2}^{\text{dilepton}}$ (GeV) >				600	600	600

Requirement	SR $3l$ -comp			SR $3l$ - \tilde{g}		
	SR-A	SR-B	SR-C	SR-A	SR-B	SR-C
E_T^{miss} (GeV) >				150	150	150
m_T^{min} (GeV) >				100	100	100
$p_T^{\ell\ell}$ (GeV) <	60	60	60	150	150	150
R >	0.45	0.5	0.55	0.55	0.6	0.65
m_{eff} (GeV)	< 500	< 500	< 500	> 650	> 650	> 650
$M_{T_2}^{\text{dijet}}$ (GeV) >	200	200	200			

The selection criteria used for the three-lepton signal region. The SR $3l$ -comp targets soft final states resulting from the electroweakino production and $3l$ - \tilde{g} targets final states from gluino production. A Z -veto is applied to both SRs.

Optimization of cuts

Distributions in the kinematic variables m_{eff} and R used in optimizing cuts



Optimization of cuts

- Based on the distributions, we set $R > 0.85$ and vary the cuts on m_{eff} such that $m_{\text{eff}} \in [200,450]$ for SR-A, $[250,450]$ for SR-B and $[250,420]$ for SR-C.

Model	\mathcal{L} for 5σ discovery at 14 TeV					
	SR $1\ell + \text{jets}$			SR $1\ell\text{-Opt} + \text{jets}$		
	SR-A	SR-B	SR-C	SR-A	SR-B	SR-C
(g)	3573	3463	2311	1477	1730	1938
(h)	4972	4884	4133	2572	2872	3212
(i)	5232	5210	4790	3131	3666	4131
(j)	6160	6089	6039	3484	3934	4385